Depletion of Phosphate in Active Muscle Fibers Probes Actomyosin States within the Powerstroke

E. Pate,* K. Franks-Skiba,# and R. Cooke#
*Department of Pure and Applied Mathematics, Washington State University, Pullman, Washington 99164, and #Department of Biochemistry and Biophysics and CVRI, University of California, San Francisco, California 94143 USA

ABSTRACT Variation in the concentration of orthophosphate (P_i) in actively contracting, chemically skinned muscle fibers has proved to be a useful probe of actomyosin interaction. Previous studies have shown that isometric tension (P_o) decreases linearly in the logarithm of $[P_i]$ for $[P_i] \geq 200$ μM. This result can be explained in terms of cross-bridge models in which the release of P_i is involved in the transition from a weakly bound, low-force actin · myosin · ADP · P_i state to a strongly bound, high-force, actin · myosin · ADP state. The 200 μM minimum $[P_i]$ examined results from an inability to buffer the intrafiber, diffusive buildup of P_i resulting from the fiber ATPase. In the present study, we overcome this limitation by employing the enzyme purine nucleoside phosphorylase with substrate 7-methylguanosine to reduce the calculated internal $[P_i]$ in contracting rabbit psoas fibers to <5 μM. At 10°C we find that P_o continues to increase as the $[P_i]$ decreases for $[P_i] \geq 100$ μM. Below this $[P_i]$, P_o is approximately constant. These results indicate that the free energy drop in the cross-bridge powerstroke is $\sim 9kT$. This value is shown to be consistent with observations of muscle efficiency at physiological temperatures.

INTRODUCTION

Chemical free energy for the production of force and work in contracting muscle is provided by the hydrolysis of ATP to ADP and orthophosphate (P_i) by the actomyosin ATPase. However, the relationships between the intermediate biochemical states in the contractile cycle and the mechanical properties of contracting muscle remain unresolved. P_i is the first hydrolysis product to be released from the actomyosin complex (reviewed, Taylor, 1979; Cooke, 1986), potentially via the large cleft in the 50K myosin domain by a "backdoor" enzymatic process (Rayment et al., 1993a,b; Yount et al., 1995). Investigations of muscle mechanics in skinned, mammalian, skeletal muscle fibers over the $[P_i]$ range 200 μM to 70 mM have shown that an increasing $[P_i]$ decreases isometric tension (P_o) linearly in the log$[P_i]$, while having little effect on maximum shortening velocity (Cooke and Pate, 1985; Hibberd et al., 1985; Kawai, 1986; Chase and Kushmerick, 1988; Pate and Cooke, 1989a; Dantzig et al., 1992; Martyn and Gordon, 1992; Millar and Homsher, 1990; Walker and Moss, 1992). These data have been taken as evidence that P_i release from the actomyosin complex is associated with the transition from a weakly bound, low-force, pre-powerstroke, A · M · ADP · P_i state (A = actin, M = myosin) to a strongly bound, high-force, A · M · ADP state (Hibberd and Trentham, 1986; Pate and Cooke, 1989a,b). The precise nature of the chemomechanical transitions involved remains unresolved (Kawai and Halvorson, 1991; Dantzig et al., 1992; Walker and Moss, 1992).

The effects of variation of the $[P_i]$ on muscle mechanics provides a probe of force-producing, powerstroke cross-bridges. Alteration of the $[P_i]$ alters the free energy differences between the various force- and non-force-producing cross-bridge states and thus yields information regarding the spatial distribution of cross-bridges within the working powerstroke. For example, analysis of the experimental data using the models of Hibberd and Trentham (1986) or Pate and Cooke (1989a,b) predicts an undiminished, continued increase in P_o for $[P_i]$ decreasing below 200 μM. This is due to the increasing free energy available from the hydrolysis of ATP, which results in a progressively longer powerstroke length, and thus an increasing fraction of ever more highly strained cross-bridges attached at the beginning of the powerstroke. Other possibilities obviously exist, however. For example, the physical length of a myosin cross-bridge could limit the ultimate strain at which cross-bridges can attach, resulting in a leveling off of the tension increase with decreased $[P_i]$. Titration plots over as wide a range of $[P_i]$ as possible are necessary to resolve questions concerning the dependence of actomyosin mechanics on the free energy of ATP hydrolysis.

The restricted range of P_i concentrations noted above has been necessitated by two factors. The limitation of $[P_i]$ to less than 70 mM in actively contracting fibers has been required to keep the ionic strength of the experimental buffers at levels below which the myosin thick filaments do not start to depolymerize. The restriction to $[P_i]$ greater than 200 μM has resulted from an inability to buffer the diffusive accumulation of P_i liberated within fiber via the actomyosin ATPase of the fiber. Attainment of even this 200 μM minimum level required the inclusion of the sucrose phosphorylase-sucrose, enzyme-substrate system in experimental buffers to reduce residual, buffer P_i contamination (primarily from commercially available phosphocreatine) to <10 μM (Pate and Cooke, 1989a; Millar and Homsher, 1990). Unfortunately, the Michaelis constant of sucrose phosphorylase for P_i is in the millimolar range (Mieyal and

Received for publication 8 July 1997 and in final form 6 October 1997.
Address reprint requests to Dr. Edward F. Pate, Department of Mathematics, Washington State University, Pullman, WA 99164. Tel.: 509-335-3151; Fax: 509-335-1188; E-mail: epate@wsu.edu.

0006-3495/98/01/369/12 $2.00

Abeles, 1972). Thus the activity of the enzyme has proved to be much too low to buffer P_i concentrations of the magnitude generated by the fiber ATPase at attainable sucrose phosphorylase concentrations.

Webb and co-workers (Webb, 1992; Brune et al., 1994) have demonstrated the potential of the enzyme nucleoside phosphorylase (NP) with substrate 7-methylguanosine to serve as a "phosphate mop" to reduce the $[P_i]$. With an equilibrium constant greater than 100, submicromolar P_i concentrations were possible in solution. In the present study, we have used this enzymatic system to buffer P_i concentrations within actively contracting fibers. Because of the inhibitory effects on NP of chemical species frequently employed in fiber studies, this has not proved as straightforward as might be anticipated. Nonetheless, we have been able to decrease calculated internal P_i concentrations in actively contracting muscle fibers to levels less than 5 μM, and have investigated the effects of decreased $[P_i]$ on isometric tension. We found that P_o increased with decreasing $[P_i]$ for $[P_i] \geq 100$ μM. Below 100 μM, a further decrease in $[P_i]$ did not significantly affect P_o. These results are considered in terms of currently popular hypotheses regarding cross-bridge function.

MATERIALS AND METHODS

Fiber mechanics

Rabbit psoas fibers were harvested and chemically skinned as described previously (Cooke et al., 1988). For mechanical experiments, single fibers were dissected from a bundle of fibers and mounted in a well between a solid-state force transducer and a rapid motor for changing fiber length. Fiber mounting and the experimental apparatus have been described in detail elsewhere (Cooke et al., 1988; Pate et al., 1991). Fiber diameter was determined taking measurements at $\times$100 magnification at four to six locations along the fiber and averaging the values.

We wished to examine the mechanical properties of fibers contracting over a range of P_i concentrations. It has previously been observed that the unbuffered $[P_i]$ within an active rabbit psoas fiber (10°C) resulting from diffusive P_i buildup from the isometric ATPase is ~200 μM (Pate and Cooke, 1989a; Millar and Homsher, 1990). Thus for a final internal $[P_i] <$ 200 μM, it was necessary to add the NP enzymatic system to experimental buffers; $[P_i] > 200$ μM could be obtained by simple addition of P_i to buffers. To minimize the diffusive buildup of hydrolysis products in experiments involving a final internal $[P_i] < 200$ μM, thinner fibers were selected from the fiber bundles at the time of dissection. Furthermore, some individual fibers were subsequently dissected into smaller-diameter bundles of myofibrils. Except as noted, the following protocols were employed. All fiber mechanics experiments were performed at pH 7.0, 10°C. After mounting, the fiber was initially washed for 2 min in a rigor buffer containing 5 mM $Mg(OAc)_2$, 40 mM 3-(*N*-morpholino)propanesulfonic acid (MOPS), 1 mM EGTA, 0.18 M KOAc to reduce to the extent possible any P_i or nucleotide contamination from the skinning solution. Mechanical measurements at low $[P_i]$ were performed by subsequently immersing the mounted fiber in a relaxing buffer containing 8.3 mM $Mg(OAc)_2$, 40 mM MOPS, 1 mM EGTA, 5.9 mM Na_2ATP (5.0 mM MgATP), 0.15 M KOAc, variable amounts of nucleoside phosphorylase (up to 440 units/ml), and sufficient added KH_2PO_4/K_2HPO_4 to yield an average internal $[P_i]$ of 200 μM upon activation. The magnitude of the P_i addition was established by solving the relevant differential equations (Materials and Methods), using the measured fiber diameter as input. This value was adjusted by the experimentally determined P_i contamination in ATP stocks (Results). The fiber was incubated in this buffer for >3 min to ensure diffusive equilibration of NP interior to the fiber. The fiber was then activated by the addition of 1.1 mM $CaCl_2$. The NP reaction was initiated by the addition of 8 mM 7-methylguanosine, and the maximum increase in tension was recorded. In determining absolute fiber tension, we have previously found that the measurement of the fiber diameter introduces the largest error. The protocol employed allowed each fiber to serve as its own control for fiber diameter. ATP is a weak inhibitor of the NP-catalyzed reaction (Results). To obtain as low a $[P_i]$ as possible, the activating buffer in some experiments involving our thinnest, dissected, myofibrilar bundles was modified to contain 3.7 mM $Mg(OAc)_2$, 0.93 mM Na_2ATP (750 μM MgATP), 0.18 M KOAc, thus reducing the concentration of the inhibitor.

For experiments requiring a final $[P_i] > 200$ μM, the protocols were similar to those we have used previously. A relaxing buffer as above (8.3 mM $Mg(OAc)_2$, 40 mM MOPS, 1 mM EGTA, 5.9 mM Na_2ATP, 0.15 M KOAc, and omitting NP) but also containing 0.15 units/ml sucrose phosphorylase, 5 mM sucrose, was allowed to sit at room temperature for 2 h before experimentation to eliminate any contaminating P_i. We have previously shown that the use of the sucrose phosphorylase system can remove low levels of contaminating P_i from buffers without being sufficiently active to substantively affect the P_i levels in the subsequent experimental steps (Pate and Cooke, 1989a). A second relaxing buffer as above was prepared containing 11.2 mM $Mg(OAc)_2$, 5.75 mM Na_2ATP (5.0 mM MgATP), with KOAc and MOPS replaced by 32.0 mM K_2HPO_4 and 45.3 mM KH_2PO_4. Intermediate concentrations (1 mM $\leq [P_i] \leq$ 77.3 mM) were obtained by linear proportional mixing of the 0 P_i buffer with this new buffer. Free Mg^{2+} concentrations were 2–3 mM in all buffers. Isometric tensions were then determined following the protocols of Pate and Cooke (1989a).

The concentrations of the various ionic species were calculated from standard binding constants as described previously (Pate et al., 1991). The pK_a for orthophosphate was taken as 6.75. The final calculated ionic strength of all activating buffers was $\mu = 210$ mM. The concentrations of the various ionic species are not linear functions of the added components. The use of linear interpolation to form buffers containing a $[P_i]$ between 1 mM and 77.3 mM resulted in $\leq$0.5% error in either the calculated $[P_i]$ or ionic strength. This small error was ignored.

Determination of nucleoside phosphorylase activity

Nucleoside phosphorylase catalyzes the reaction 7-methylguanosine + $P_i \leftrightarrow$ 7-methylguanine + ribose-1-phosphate. Under the conditions employed in these studies, the equilibrium is strongly to the right. Except as subsequently noted, NP activity was determined using an experimental buffer containing 5 mM $Mg(OAc)_2$, 40 mM MOPS, 1 mM EGTA, 1.1 mM $CaCl_2$, 0.18 M KOAc, 0.04–2.0 units/ml nucleoside phosphorylase and variable concentrations of 7-methylguanosine, ribose-1-phosphate, K_2HPO_4/KH_2PO_4, ATP, and ADP, pH 7.0, 10°C, $\mu = 210$ mM. The reaction was initiated by the addition of P_i. The change in fluorescence associated with the conversion of 7-methylguanosine to 7-methylguanine was monitored with the temperature-controlled fluorimeter previously described (Franks-Skiba et al., 1994), with $\lambda_{exc} = 300$ nm, $\lambda_{obs} = 400$ nm, and a slit width of 2.5 mm. After generation of a plot of the linear decrease in fluorescence as a function of time ($\Delta t > 1$ min), excess P_i and NP were added to the reaction cuvette. The reaction was allowed to go to completion, and the final fluorescence level was determined. 7-Methylguanine has a small but nontrivial intrinsic fluorescence under the experimental conditions (Kulikowska et al., 1986). Activity was calculated based on the proportional decrease in fluorescence during the period of linear decrease, adjusting for the final fluorescence level. Additional compensations were made for the small fluorescences of the enzyme, ATP, and ADP, and for dilution factors resulting from the sequential addition of experimental buffer components to the fluorimeter cuvette. Further details are provided in Results. Nucleoside phosphorylase ("bacterial"), 7-methylguanosine, ATP, ADP, ribose-1-phosphate, creatine phosphate, and phosphoenolpyruvate were purchased from Sigma Chemical Co. Nucleoside phosphorylase

was dialyzed against a 1000-fold excess of the experimental buffer for 10 h before use.

Kinetic data were fit to a bimolecular, saturation function, assuming that ATP, ADP, and ribose-1-phosphate functioned as classical competitive inhibitors (via modification of the Michaelis constants),

$$V_{mN}/V = K_{mNP}(1 + A/K_{iPA} + D/K_{iPD} + R/K_{iPR})(1/P) + K_{mNM}(1 + A/K_{iMA} + D/K_{iMD} + R/K_{iMR})/(1/M) + 1 \quad (1)$$

Here, P, M, R, A, and D are the concentrations of P_i and 7-methylguanosine, ribose-1-phosphate, ATP, and ADP, respectively. V_{mN} is the velocity of NP at simultaneously infinite concentrations of P_i and 7-methylguanosine. K_{mNP} and K_{mNM} are the respective Michaelis constants for P_i and 7-methylguanosine. K_{iPA}, K_{iPD}, and K_{iPR} are the P_i inhibition constants, with the third subscript denoting the competing species; similarly, K_{iMA}, K_{iMD}, and K_{iMR} are the 7-methylguanosine inhibition constants. A least-squares minimization of Eq. 1 to the aggregate enzyme velocity data was used to establish the values for K_{iPA}, K_{iPD}, K_{iPR}, K_{iMA}, K_{iMD}, K_{iMR}, V_{mN}, K_{mNP}, and K_{mNM} that were used in the modeling analyses to approximate the [P_i] internal to contracting fibers. A reciprocal format was chosen for the fittings to more heavily weight the kinetic velocity data at low [P_i], because this is the regimen of greatest interest in this study.

Determination of the [P_i] internal to contracting fibers

To approximate the internal [P_i], we use an extension of a modeling approach previously employed to investigate substrate concentrations within active fibers (Cooke and Pate, 1985; Pate and Cooke, 1989a). Internal [P_i] in contracting fibers is determined by three factors: 1) the P_i produced by the fiber actomyosin ATPase; 2) the P_i that is eliminated by the NP-catalyzed reaction; and 3) the diffusion of P_i out of the fiber into the surrounding experimental buffer. Thus we need balance laws describing the diffusion and chemical interaction within the fiber of the species involved in the fiber ATPase and the NP-catalyzed reaction. Assume a fiber to be cylindrical, with $r \geq 0$ designating the spatial distance from the center of the fiber. Let $T(r)$, $D(r)$, $P(r)$, $M(r)$, $R(r)$, and $m(r)$ be the steady-state in time, radially dependent, internal concentrations of ATP, ADP, P_i, 7-methylguanosine, ribose-1-phosphate, and 7-methylguanine, respectively. Then at equilibrium, for $0 \leq r < a$,

$$\begin{aligned}
&C_T\nabla^2 T(r) - k_A[T(r), D(r)] = 0\\
&C_D\nabla^2 D(r) + k_A[T(r), D(r)] = 0\\
&C_P\nabla^2 P(r) + k_A[T(r), D(r)] - \rho_N v_f k_N[T(r), D(r), P(r), M(r), R(r), m(r)] = 0\\
&C_M\nabla^2 M(r) + \rho_N v_f k_N[T(r), D(r), P(r), M(r), R(r), m(r)] = 0\\
&C_R\nabla^2 R(r) + \rho_N v_f k_N[T(r), D(r), P(r), M(r), R(r), m(r)] = 0\\
&C_m\nabla^2 m(r) + \rho_N v_f k_N[T(r), D(r), P(r), M(r), R(r), m(r)] = 0
\end{aligned} \quad (2)$$

with the additional boundary condition that the concentrations are the external bath values at the fiber surface, $r = a$: $T(a) = T_0$, $D(a) = D_0$, $P(a) = P_0$, $M(a) = M_0$, $R(a) = R_0$, $m(a) = m_0$. Here, ∇^2 is the Laplacian in cylindrical coordinates, $d^2/dr^2 + r^{-1}\, d/dr$; C subscripted with T, D, P, M, R, or m is the appropriate diffusion coefficient; ρ_N is the concentration of NP; v_f is the volume fraction internal to the fiber that is available to NP; and the functions k_A and k_N give the rates of the fiber ATPase and the NP-catalyzed reactions. We assume that the fiber ATPase exhibits classical saturation kinetics, with ADP as a competitive inhibitor, and take (Cooke and Pate, 1988)

$$k_A[T, D] = \frac{\rho_m V_{mA} T}{K_{mA}(1 + D/K_{iD}) + T} \quad (3)$$

where ρ_m is the concentration of myosin in the fiber, V_{mA} is the maximum ATPase rate at infinite [ATP], K_{mA} is the Michaelis constant, and K_{iD} is the ADP inhibition constant. Here our kinetic data (Results) indicate that as a first approximation, species appear to function as classical, competitive inhibitors of NP, and we take

$$k_N[T, D, P, M, R, m] = \frac{V_{mN} PM}{K_{mNP}(1 + A/K_{iPA} + D/K_{iPD} + R/K_{iPR} + m/K_{iPm})P + K_{mNM}(1 + A/K_{iMA} + D/K_{iMD} + R/K_{iMR} + m/K_{iMm})M + PM} \quad (4)$$

Equation 4 is equivalent to Eq. 1, with the inclusion of 7-methylguanine as a competitive inhibitor (inhibition constants, K_{iPm} and K_{iMm}, for P_i and 7-methylguanosine, respectively). The limitations of this approximation will be considered subsequently (Discussion).

The following parameter values from the literature were used: $C_P = 2.1 \times 10^{-6}$ cm^2/s (Yoshizaki et al., 1982); $C_A = 2 \times 10^{-7}$ cm^2/s (Mannherz, 1968; Marston, 1973); $\rho_m = 220$ μM (Franks and Cooke, 1980); $V_{mA} = 1.3$/s/myosin head (Cooke et al., 1988); $K_{mA} = 20$ μM (Sleep and Glyn, 1986); $K_{iD} = 250$ μM (Cooke and Pate, 1985; Sleep and Glyn, 1986). C_D and C_M were taken as equal to C_A; C_m and C_R were taken as 4×10^{-7} cm^2/s, assuming that the effective Stokes-Einstein radii of the products were 50% that of the other triphosphate species. K_{iMR} and $K_{iMm} = 0.5$ mM, a lower limit determined by Kulikowska et al. (1986). Other values are determined in the Results.

For every fiber for which data were collected, the radius, a, was determined. With knowledge of the fiber bath concentrations, Eq. 2 was then solved as a two-point, boundary value problem with finite differencing of the derivative terms. The singularity in the Laplacian at the origin was handled by noting that l'Hôpital's rule implies that $r^{-1}\, d/dr \rightarrow d^2/dr^2$ as $r \rightarrow 0$. The solution of the resulting system of nonlinear, algebraic equations for the concentrations of the six chemical species at the mesh points was obtained using Newton's method. The average [P_i] was then approximated by evaluating $(1/\pi a^2)\int_0^a P(r) r\, dr$, where a is the fiber radius.

In the analysis of some experimental protocols, the time evolution of the various species were of interest and diffusion could be ignored to a first approximation. Here the following system of equations was employed:

$$\begin{aligned}
dP(t)/dt &= -\rho_N v_f k_N[T, D, P, M, R, m]\\
dM(t)/dt &= -\rho_N v_f k_N[T, D, P, M, R, m]\\
dR(t)/dt &= \rho_N v_f k_N[T, D, P, M, R, m]\\
dm(t)/dt &= \rho_N v_f k_N[T, D, P, M, R, m]
\end{aligned} \quad (5)$$

where $P(t)$, $M(t)$, $R(t)$, and $m(t)$ are now the time-dependent, spatially uniform concentrations of P_i, 7-methylguanosine, ribose-1-phosphate, and 7-methylguanine.

RESULTS

Nucleoside phosphorylase activity

There have been extensive investigations of the interaction of nucleoside phosphorylases with numerous chemical species. The facts that 1) the experimental conditions used to study the NP-catalyzed reaction frequently differ from those used in fiber physiology studies; 2) some of the species used in fiber studies have previously been suggested to inhibit NP; 3) in the course of the fiber studies we determined that

creatine phosphate was an extremely effective inhibitor of NP; and 4) we shall use a modeling approach to approximate the [P_i] internal to fibers all suggested the necessity of running control experiments on enzyme activity. Fig. 1 shows the protocol used to measure enzymatic activity. The reaction buffer (minus enzyme, P_i, and 7-methylguanosine) was placed in the fluorimeter cuvette. After stabilization of the signal, enzyme and 7-methylguanosine were sequentially added, with sufficient time between additions to ensure a stable signal. The reaction was initiated by the addition of P_i, and the signal was followed for $\Delta t > 1$ min. Excess P_i and enzyme were then added; the reaction was allowed to go to completion; and then additional enzyme was added to monitor the intrinsic fluorescence of the enzyme. As is evident, the slightly elevated fluorescence after completion of the reaction results primarily from the small fluorescence of 7-methylguanine under the experimental conditions. Proportional weighting was used to compensate for this in the determination of activity as given by the slope of the linearly decreasing fluorescence after the initial addition of P_i.

We investigated the inhibition of the NP-catalyzed reaction by ATP, ADP, and ribose-1-phosphate. Commercially available ATP, ADP, and ribose-1-phosphate all contain contaminating, free P_i. These levels were determined as above by using 2 units/ml NP, except that P_i was omitted from the experimental buffer. Instead, the reaction was initiated by the addition of 150 μM ribose-1-phosphate, 5 mM ATP, or 5 mM ADP and allowed to proceed until no additional decrease in fluorescence with time could be observed ($\Delta t > 5$ min). The [P_i] was raised to 5 mM; the reaction was again allowed to go to completion; and proportional decreases were then used to calculate the P_i contamination. The percentage P_i contaminations (mean $\pm$ SE) obtained were 5.9 $\pm$ 0.07% (five observations) for ribose-1-phosphate, 0.12 $\pm$ 0.01% (four observations) for ATP, and 0.08 $\pm$ 0.01% (six observations) for ADP. Experimental P_i concentrations were adjusted by these amounts in competition experiments involving ATP or ADP. A similar adjustment was made in fiber experiments for substrate contamination.

Fig. 2 *A* gives double-reciprocal plots of 1/(reaction velocity) versus 1/[P_i] at a 150 μM concentration of 7-methylguanosine in the presence of 0.2 mM ribose-1-phosphate (◇), 1.5 mM ATP (△), 0.5 mM ADP (□), and in the absence of inhibitor (○). Fig. 2 *B* gives a similar double-

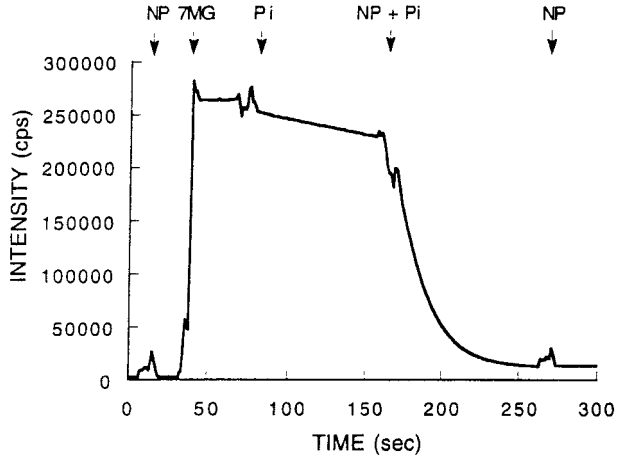

FIGURE 1 Fluorescence intensity as a function of time for a determination of enzymatic activity. After sequential additions of 0.04 units/ml nucleoside phosphorylase (*arrow NP*) and 300 μM 7-methylguanosine (*arrow 7MG*) to the reaction buffer, the reaction is initiated by the addition of 300 μM P_i (*arrow Pi*). The brief deviations in the plot at the time of the additions are artifacts resulting from the fluorimeter cavity cover being open during component addition and stirring. The decrease in fluorescence is followed for sufficient time to determine a reaction rate. Excess P_i (2 mM) and enzyme (0.6 units/ml) (*arrow NP + Pi*) are added and the reaction is allowed to go to completion. An additional 0.6 units/ml of enzyme (*arrow NP*) is finally added to monitor the intrinsic fluorescence of the enzyme. The activity determined from the slope is proportionally adjusted to account for the higher final fluorescence. Additional details are in Materials and Methods.

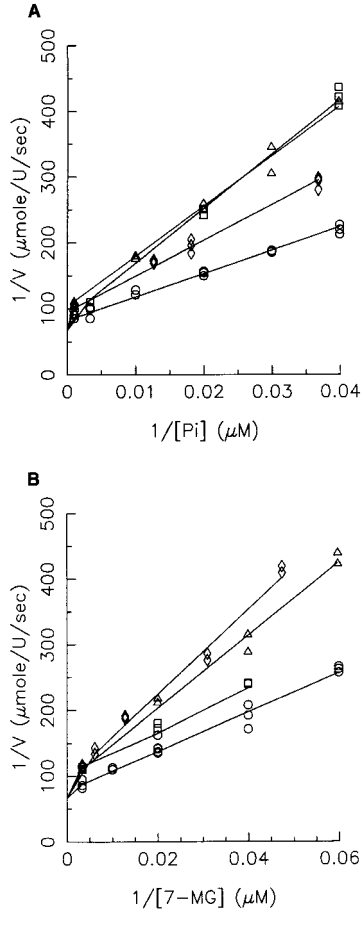

FIGURE 2 Double reciprocal plots of (reaction velocity)$^{-1}$ versus [substrate]$^{-1}$. (*A*) The reaction buffer contained variable [P_i], a fixed 150 μM concentration of 7-methylguanosine (○). Data are also shown for the addition of 0.2 mM ribose-1-phosphate (◇), 1.5 mM ATP (△), or 0.5 mM ADP (□) to the reaction buffer. (*B*) The reaction buffer contained variable 7-methylguanosine, a fixed 300 μM concentration of P_i (○), with the addition of 0.5 mM ribose-1-phosphate (◇), 1.5 mM ATP (△), or 1.5 mM ADP (□). Solid lines are the least-squares fit of all data to the nonlinear Eq. 1.

reciprocal plot for variable concentrations of 7-methylguanosine at 300 μM P_i, 0.5 mM ribose-1-phosphate (◇), 1.5 mM ATP (△), ADP (□), and in the absence of inhibitor (○). The solid lines show that the data are well fit by Eq. 1. The least-squares values obtained over all data yield a V_{max} for the enzyme of $V_{mN} = 0.15$ μmol/unit/s and Michaelis constants of $K_{mNP} = 49.2$ μM and $K_{mNM} = 44.4$ μM for P_i and 7-methylguanosine, respectively. The inhibition constants for ribose-1-phosphate, ATP, and ADP at the P_i site were $K_{iPR} = 316$ μM, $K_{iPA} = 1.15$ mM, and $K_{iPD} = 333$ μM, respectively. The inhibition constants for ribose-1-phosphate, ATP, and ADP at the 7-methylguanosine site were $K_{iMR} = 430$ μM, $K_{iMA} = 1.74$ mM, and $K_{iMD} = 5.8$ mM. Standard errors for the nonlinear fit to the parameters were 9–14% of the calculated values.

The important observation for the present studies is that these controls yielded values in the ranges suggested by previous investigators. The values for the Michaelis constants suggested by our studies at low temperature (10°C) and physiological pH and ionic strength were in the range previously determined by Brune et al. (1994). In those studies, the Michaelis constant for 7-methylguanosine was 59 μM and that for P_i was 34 μM at pH 8.0, low ionic strength, and high temperature (30°C). Assuming a molecular weight of 120,000 for the enzyme, and that the commercially obtained product is one-third active (Brune et al., 1994), this equivalently defines $V_{mN} = 39\ s^{-1}$, again comparable to the value of 104 s^{-1} obtained by Brune et al., when the differences in temperature are taken into account. Porter (1992) has previously suggested a K_i of ~100 μM for ribose-1-phosphate for NP from calf spleen. Assuming a substrate K_m of 50 μM, the data of Murakami et al. (1971) suggest a similar effective K_i for ADP binding to NP from chicken liver. Pyrimidine triphosphates bind to bovine spleen NP with a K_i of 100–200 μM (Ropp and Traut, 1991). Inhibition constants for various NP isoforms in the range of >0.25 mM have previously been reported for purine species (Krenitsky et al., 1968; Zimmerman et al., 1971; Kulikowska et al., 1986). One exception to the values reported here, and based on more limited observations under different conditions, is the report of Brune et al. (1994) that ATP binds 3000 times less strongly than P_i. Given the availability of a single set of kinetic observations under a relevant set of experimental conditions, our calculations of the [P_i] within a muscle fiber will use the kinetic values measured here and given above. The implications of the observation of Brune et al. will be addressed in Materials and Methods. Furthermore, the quality of the fit of the data to Eq. 1 suggests our assumption of classical competitive inhibition to be a reasonable first approximation to the enzyme kinetics.

To calculate the [P_i] within a muscle fiber in the presence of the NP-catalyzed reaction, it is also necessary to know the internal volume fraction of a fiber that is accessible to NP (v_f, Eq. 2). This is the proportional decrease in the reaction rate at a given NP concentration. The following protocol was used to determine v_f. Bundles of ~25 fibers were incubated on ice for 12 h in a 500-fold excess of the buffer used for kinetic experiments (Materials and Methods), containing 0 mM 7-methylguanosine, 0 mM P_i, and 400 units/ml NP, to allow for diffusive equilibration of NP interior to the fibers. The fiber bundles were then removed from the buffer and carefully blotted to remove excess buffer. The fiber bundle volume was determined by weight. The fibers were then placed in a 200-fold excess of the above buffer, 0 units/ml NP. The fibers were then briefly sonicated at 0°C and allowed to equilibrate at 0°C for 2 h. The fiber mixture was centrifuged to remove the fiber debris, and the NP activity of the supernatant was assayed as previously described, using 150 μM 7-methylguanosine, 300 μM P_i as the substrate. This activity was compared to that produced by a buffer that contained 400 units/ml NP and no fibers, but which was still allowed to undergo the incubations. The reduced activity from the fiber supernatant defined $v_f = 0.64 \pm 0.04$ (mean ± SE, five observations). We note that this value for v_f is virtually identical to the previously determined value of $v_f = 0.62$ determined from the volume fraction available for the diffusion of electron paramagnetic resonance spin-labeled hemoglobin into fibers (Pate and Cooke, 1988). The volume of a skinned fiber is ~80% water. Approximately 20% of the intracellular water is excluded from the diffusion of electrolytes (reviewed in Cooke and Kunz, 1974). Thus the volume fractions available to NP and the other buffer components are roughly equivalent.

Effects of ATP-regenerating systems on nucleoside phosphorylase activity

During the course of these studies it became apparent that in addition to nucleotide, other chemical species that are commonly employed in experimental buffers for fiber mechanics experiments were competitive inhibitors of the NP-catalyzed reaction. Fig. 3 shows the influence of creatine phosphate on the reaction. The reaction was initiated as in Fig. 1 (300 μM P_i, 300 μM 7-methylguanosine, 0.06 units/ml NP). At point CP, 5 mM creatine phosphate was added. As is evident, the NP reaction rate became virtually zero. Creatine phosphate concentrations of ≥20 mM are required to buffer ATP concentrations internal to fibers in mechanical experiments under the conditions we are using in the present experiments (Cooke and Bialek, 1979). Thus the data of Fig. 3 indicated that the addition of useful levels of creatine phosphate in buffers would prevent us from reducing internal P_i concentrations with NP. The data of Fig. 3, along with other observations at lower creatine phosphate concentrations, indicated that millimolar creatine phosphate had a surprisingly low effective K_i of <75 μM. An alternative method for buffering internal substrate concentrations was through the use of the pyruvate kinase-phosphoenolpyruvate system. P_i contamination in phosphoenolpyruvate was determined to be 0.77 ± 0.18% (nine observations). Using this value, we found an effective K_i for

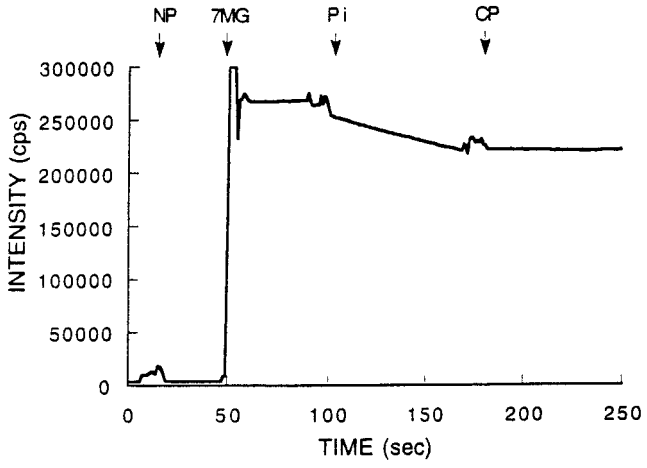

FIGURE 3 The decrease in fluorescence after initiation of the nucleoside phosphorylase catalyzed reaction is monitored as in Fig. 1. Conditions: 0.06 units/ml nucleoside phosphorylase, 300 μM P_i, 300 μM 7-methylguanosine. At the arrow marked CP, 5 mM creatine phosphate is added, resulting in a dramatic decrease in reaction velocity.

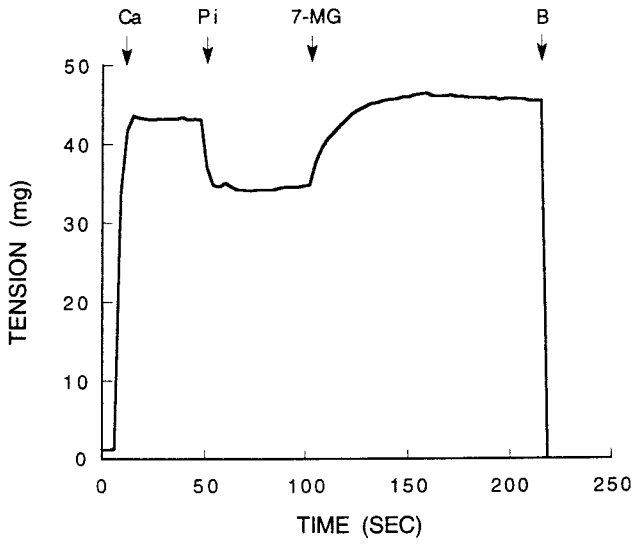

FIGURE 4 A representative experiment showing the effects of the nucleoside phosphorylase catalyzed reaction on fiber mechanics. At the arrow Ca, a mounted fiber is activated in a buffer containing 5 mM MgATP, 4.5 units/ml nucleoside phosphorylase, 0 mM 7-methylguanosine, with buffer P_i adjusted to yield an internal calculated fiber $[P_i]$ of 200 μM. At the arrow denoted P_i, 0.8 mM P_i is added. The final average $[P_i]$ internal to the fiber is now 1 mM, and the isometric tension decreases, as has previously been observed. At the arrow denoted 7-MG, 8 mM 7-methylguanosine is added. The relative fiber tension increases to a value above that obtained at 200 μM $[P_i]$ as the calculated $[P_i]$ internal to the fiber decreases to 129 μM. At arrow B, the fiber was broken to check for baseline drift. Fiber diameter = 58.7 μm.

phosphoenolpyruvate of 800 μM (data not shown), again much too low a value to enable the pyruvate kinase-phosphoenolpyruvate system to be employed in our fiber studies. A complete analysis of the inhibition of the NP-catalyzed reaction by creatine phosphate and phosphoenolpyruvate is obviously beyond the scope of the present manuscript. Fig. 3 and the observations on phosphoenolpyruvate are included simply to alert other fiber mechanics researchers to potential artifacts when NP is employed.

Fiber mechanics

Because of the above-noted inhibition of NP by the components of commonly used ATP regenerating systems, it was decided to perform experiments in the absence of any ATP-regenerating system. Fig. 4 demonstrates our principal result: the efficacy of the NP system in intact fibers. A fiber was mounted in the relaxing buffer as described in Materials and Methods (4.5 units/ml NP), with buffer P_i adjusted so that the model equations for the $[P_i]$ internal to the fiber (see Materials and Methods and below) gave an average internal $[P_i]$ immediately after activation of 200 μM. After activation by the addition of Ca^{2+}, 0.8 mM P_i was added to the buffer to raise the total internal fiber P_i to 1 mM. Tension decreased by 20%. 7-Methylguanosine at a concentration of 8 mM was subsequently added to initiate the NP-catalyzed reaction. As can be seen, tension rose by 36% in a time period of ~50 s, with the final tension above the initial isometric level obtained before the initial addition of 0.8 mM P_i. After the addition of 7-methylguanosine, the final internal calculated $[P_i]$ decreased to 129 μM. The decrease in fiber tension upon the initial increase in the $[P_i]$ to 1 mM was compatible with previous observations in this laboratory (Pate and Cooke, 1989a). The tension increase after the addition of 7-methylguanosine to the reaction buffer was comparable to that obtained with other fibers. This is demonstrated in Fig. 6, where the points denoted by solid diamonds give the tension values for the fiber of Fig. 4, relative to the tension value obtained at 200 μM P_i. In all other experiments, a final $[P_i] < 200$ μM was achieved using the previously described protocols (Materials and Methods), with fibers activated under conditions yielding a calculated internal $[P_i] = 200$ μM.

In all of these experiments, the final $[P_i]$ was determined by solving the appropriate diffusive balance law for the species concentrations and fiber diameter involved (Eqs. 2–4). Fig. 5 gives representative solution concentrations for a fiber of measured diameter 49.6 μm, 200 units/ml NP. Fig. 5 *A* gives the concentrations of ATP, ADP, 7-methylguanosine, ribose-1-phosphate, and 7-methylguanine internal to the fiber as a function of the distance, *r*, from the fiber center. The profiles are roughly parabolic in *r*, as expected (Cooke and Pate, 1985). Fig. 5 *B* demonstrates the effect of the presence of NP, giving the $[P_i]$ as a function of *r* on the assumption of 0 units/ml NP (*dashed line*) and 200 units/ml (*solid line*). The average $[P_i]$ was reduced to a calculated value of 33.2 μM above the ambient buffer level in the presence of NP. With an equilibrium greater than 100 (Brune et al., 1994), the ambient level was less than 0.6 μM.

Fig. 6 shows the accumulated data of tension versus $\log[P_i]$. Open circles give the data we have obtained using

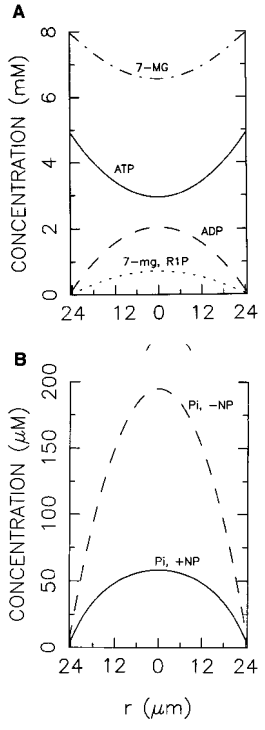

FIGURE 5 Species concentrations as a function of the distance r from the center of a 24.8 μm-radius fiber determined by solution of Eqs. 2–4 with the following concentrations (mM) in the experimental buffer: ATP = 5, ADP = 0, P_i = 0, 7-methylguanosine = 8, ribose-1-phosphate = 0, 7-methylguanine = 0. Nucleoside phosphorylase concentration was 200 units/ml. (*A*) All species except P_i. Average concentrations (mM): ATP = 3.97, ADP = 1.03, 7-methylguanosine = 7.32, ribose-1-phosphate = 0.34, 7-methylguanine = 0.34. (*B*) P_i concentrations in the presence (——) and absence (– – –) of 200 units/ml nucleoside phosphorylase. The effect of nucleoside phosphorylase is evident. The average [P_i] in the presence of nucleoside phosphorylase is 33.2 μM. The observed tension increase by this fiber when the [P_i] is reduced from 200 μM to 33 μM is shown by the data point marked with a closed square in Fig. 6. Numerical solutions for the concentration profiles of other fibers used in these studies are available upon request.

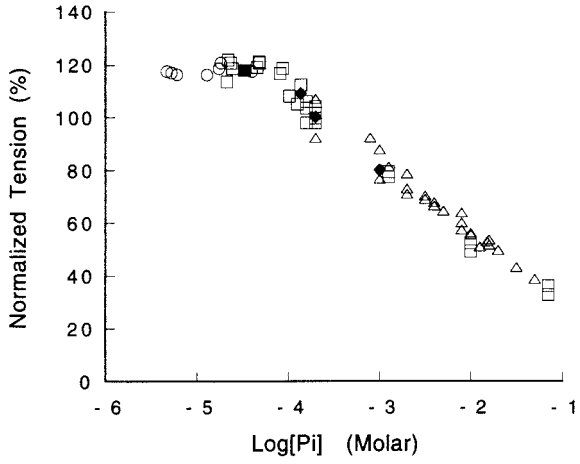

FIGURE 6 Tension relative to that obtained at 200 μM P_i as a function of log[P_i]. ○, Split fibers; □, fibers that have not been split; ■, fiber of Fig. 5; ◆, fiber of Fig. 4. The open triangles are normalized data from other studies as described in the text.

fibers that have been split into thinner segments. Open squares give data from unsplit fibers. We note that there is an overlap region where both protocols yield the same result. The solid diamonds are from the fiber of Fig. 4, and the solid square is from the fiber of Fig. 5. In the figure, final concentrations of $P_i > 200$ μM were obtained by the addition of P_i to activating buffers as described in Materials and Methods. The open triangles are data from other experimental studies normalized with respect to tensions obtained at P_i concentrations equivalent to those obtained in the present study (Altringham and Johnston, 1985; Kawai et al., 1987; Pate and Cooke, 1989a; Millar and Homsher, 1990; Kawai and Halvorson, 1991; Dantzig et al., 1992; Martyn and Gordon, 1992). The important observation is that the aggregate data show quite remarkable consistency between the results we have obtained in the present study at higher concentrations of P_i (> 200 μM) and those previously observed by others and by ourselves.

DISCUSSION

In the present study we have investigated the effects of variation in [P_i] on isometric tension in fast skeletal muscle. By using the enzyme NP with substrate 7-methylguanosine in experimental buffers, we have been able to reduce the internal [P_i] of actively contracting muscle fibers to a calculated value of less than 5 μM. This is an ~40-fold lower concentration than the 200 μM minimum [P_i] that was previously achieved using a less potent enzyme system to buffer internal [P_i]. These previous studies have shown that P_o increases with decreasing [P_i]. We found that as the [P_i] decreased below 200 μM, P_o continued to increase for [P_i] greater than ~100 μM. For P_i concentrations less than 100 μM, there was no further increase in P_o accompanying a decrease in [P_i].

One primary, and confounding, observation of this investigation was that the enzyme nucleotide phosphorylase was inhibited by ATP, ADP, and a number of ligands such as creatine phosphate and phosphoenolpyruvate, which are commonly included in studies of fiber physiology to replenish substrate levels within a fiber. This problem was solved by using unbuffered levels of substrate that still maintained adequate profusion within the fiber, high concentrations of NP, and thinner fibers to alleviate both the buildup of phosphate within the fiber and the depletion of ATP. In effect the ability of NP to function as a "phosphate mop" in studies of fiber mechanics is strongly dependent on the conditions in the assay.

Our method for determining the [P_i] internal to the fibers has been to use the biochemical and biophysical parameters affecting the [P_i] and then to solve the appropriate equations describing the balance of affectors. We have previously used this approach (Cooke and Pate, 1985; Pate and Cooke, 1989a) to approximate ATP, ADP, and P_i concentrations within actively contracting fibers. In the present study, the additional complexity resulting from the presence of the

NP-catalyzed reaction necessitated further evaluation of the validity of our approach. In particular, were the P_i concentrations as low as reported in Fig. 6?

The data of Fig. 4 are the most important control in this respect. Here, tension decreased for a few seconds after the initial addition of P_i, and then increased for ~50 s after initiation of the NP reaction. The decrease in tension showed that the time required for diffusive equilibration of P_i across a fiber, and the time required for the interaction of cross-bridges with P_i to modify tension were both rapid compared to the 50-s time course for the NP reaction. Thus to a first approximation, we may ignore the time constants associated with diffusion and the cross-bridge–P_i interaction in analyzing the time course of the increase in tension in Fig. 4, and use the time-dependent ordinary differential equations (Eq. 5, Materials and Methods) to approximate species concentrations. The initial $[P_i]$ is taken as 0.87 mM, the total added to bring the internal $[P_i]$ to 1 mM for the fiber of Fig. 4 before initiation of the NP reaction by the addition of 8 mM 7-methylguanosine. Solving Eq. 5 with parameters appropriate for the experimental buffer surrounding the fiber ($\rho_N = 4.5$ units/ml, $v_f = 1$, $M(0) = 8$ mM, $R(0) = m(0) = 0$ mM, $T = 5$ mM, $D = 0$ mM) yielded a calculated time interval of 43 s in which the initial added P_i is reduced to <10 μM. When we adjusted the values of ATP, ADP, 7-methylguanosine, ribose-1-phosphate, 7-methylguanine, v_f, and ρ_N to reflect instead the average values interior to the fiber in Fig. 4 (3.6 mM, 1.4 mM, 7.95 mM, 24 μM, 24 μM, 0.64, and 4.5 units/ml, respectively, as determined from the solution of Eqs. 2–4), an otherwise identical calculation yielded 85 s for the time required to decrease the $[P_i]$ to <10 μM. The 43-s value for the experimental buffer was similar to the experimentally observed 50 s required for a tension increase. The calculated 85-s value was slightly greater. The important point is that it is the $[P_i]$ interior to the fiber that actually determines isometric tension. Thus our analysis of the transient in Fig. 4 via Eq. 5 (others not shown) indicated that in our modeling, we were actually underestimating the rate of P_i elimination interior to the fiber by ~50%, and that the $[P_i]$ interior to the fibers was actually less than our calculated values. This does not affect our basic conclusion regarding the shape of the plot of P_o versus $\log[P_i]$ at low $[P_i]$. We additionally note that it was simulations like the preceding, exhibiting greatly retarded times for tension recovery in the presence of NP, that ultimately led us to the conclusion that phosphocreatine and phosphoenoylpyruvate were inhibitors of NP.

An alternative approach for examining the influence of potential errors in determining the activity of NP is to consider the effect of the NP reaction on the experiment that gave our lowest calculated internal $[P_i]$ (4.3 μM). This value was obtained by solving Eqs. 2–4 for a fiber of diameter 16.1 μm (split from a larger fiber), with the experimental buffer containing 306 units/ml NP, 8 mM 7-methylguanosine, 0.75 mM MgATP. At the extreme—if one estimates the internal $[P_i]$ by using the most conservative possible assumption that the velocity of the NP reaction was exactly zero—the calculated average $[P_i]$ increases by a factor of 2.5 to only 10.6 μM. The previously stated 200 μM internal value for the $[P_i]$ was based on a fiber of ~70-μm diameter. The dramatic reduction in calculated $[P_i]$ in the thinner fiber preparation is due to the fact that in a diffusive situation, average concentration is proportional to the square of the fiber radius (Cooke and Pate, 1985; Pate and Cooke, 1989a). Thus the approximately fourfold reduction in fiber radius to 16 μm was magnified into a 16-fold reduction in the average internal $[P_i]$. The important observation, however, is that although the presence of the "phosphate mop" components of the buffer guarantees extremely low ambient P_i levels, and allows an additional 2.5-fold decrease in our calculated internal $[P_i]$ (0.4 log units), even the assumption of zero NP activity alters our lowest $[P_i]$ by <10 μM. Again, however, these effects are too small to alter our fundamental conclusion regarding a leveling off of the increase in tension for a reduction to sufficiently low $[P_i]$.

Several additional potential sources of error need to be addressed. In these experiments, we have been able to buffer P_i levels interior to fibers, but are no longer buffering ATP and ADP levels. Fiber velocity experiments using rabbit psoas muscle at low [MgATP] have indicated that P_i competes with MgATP only very weakly, with a K_i of 80 mM (Pate and Cooke, 1989a). As is evident from Fig. 5, significant gradients of ATP and ADP can develop across fibers. Do the MgATP levels interior to fibers decrease to values at which competition could occur, altering our conclusions on the internal $[P_i]$ via the ATPase rate? In some experiments, external MgATP concentrations were decreased from 5 mM to 0.75 mM. These experiments would be the most susceptible to competition artifacts. We note, however, that this reduction in substrate was employed only for experiments involving the very thinnest dissected myofibrilar bundles, and hence the lowest P_i levels (<15 μM) examined in these studies. Because of the reduced diffusion path to the exterior bath, the minimum calculated MgATP concentration at any location within these fibers was greater than 0.5 mM for all of the experiments. The K_m for the fiber ATPase is 20 μM (Sleep and Glyn, 1986). From the K_i above, it is clear that P_i is not reducing the ATPase to any measurable extent. Increasing the [ADP] within a fiber to millimolar levels increases P_o by 15–25% (Cooke and Pate, 1985; Kawai and Halvorson, 1989; Seow and Ford, 1997). However, because our concentrations of P_i are too low to have any measurable influence on internal ADP levels through the fiber ATPase, ADP levels will be identical in a given fiber before and after initiation of the NP-catalyzed reaction. Thus to a first approximation, our experimental protocol of recording the ratio of tensions from a single fiber before and after the start of the NP-catalyzed reaction normalizes out any influence of varying ADP concentrations on the absolute values of fiber tensions.

The muscle filament lattice has negative charge. Thus the $[P_i]$ interior to a fiber could be influenced by Donnan potential effects. The Donnan potential has been measured

(Naylor et al., 1985) in rabbit psoas muscle to be 4.7 mV (0.44 kJ/mol). This was for μ = 140 mM, close to the ionic strength used in these studies. Then the equilibrium $[P_i]_{interior}/[P_i]_{exterior} = \exp(-0.44/2.5) = 0.84$. On a a logarithmic scale as in Fig. 6, this will result in all concentrations being shifted slightly to the left by ~0.08 units.

We have used an analytical method to approximate P_i concentrations internal to the fibers. Admittedly, the number of terms used to determine the [P_i] in Eqs. 2 and 4 was excessive because the concentration profiles in Fig. 5 revealed that many of the species had no substantive influence on the calculated [P_i]. However, it was necessary to initially include them to actually verify their lack of an effect, and they were simply retained in the final analyses. Brune et al. (1994) have suggested that ATP competes significantly less effectively than we have observed. When their value is used, the NP system becomes slightly more effective at eliminating P_i, and our lowest calculated [P_i] decreases from 4.3 μM to 3.9 μM. Again, it is clear that this difference produces too small an effect to alter our fundamental conclusions.

Despite the problems introduced by inhibition of the NP, our protocol allowed us to reduce phosphate levels interior to actively contracting fibers to a level more than 40-fold lower than those obtained in previous investigations. The range of phosphate concentrations attainable allows us to conclude that P_o continues to increase until the [P_i] is reduced to ~100 μM. Below ~100 μM P_i, we find that further decreases in [P_i] have no statistically significant effect on P_o. Using 100 μM P_i as a convenient partition value, there are 18 data points on the low [P_i] plateau in Fig. 6 (10 of these with [P_i] less than 25 μM) defining a maximum value for P_o of 1.17 ± 0.01 (mean ± SE, 18 observations) times the value for P_o obtained at 200 μM P_i (0.20 ± 0.02 N/mm^2, mean ± SE, 21 observations). As an additional test of the biphasic nature of the plot, we note that if a single linear regression fit of data collected in this study is compared to a biphasic linear fit with 100 μm P_i as the break point, the latter fit gives a mean square deviation that is fourfold less than than that obtained for a single regression line fit.

Skinned muscle fibers are known to be less stable mechanically than living fibers. This could be especially true for the smaller, dissected myofibrilar bundles employed in these experiments. Thus an alternative explanation for the observed leveling off of P_o for sufficiently low P_i concentrations is that mechanical instability prevents contracting fibers from yielding tensions higher than observed. However, we have previously investigated P_o in active rabbit psoas fibers as a function of temperature under similar buffer conditions (Pate et al., 1994). In that study, isometric tensions of 0.29 N/mm^2 could be reproducibly obtained (30°C). This value is 24% higher than the maximum tensions observed in the present study, suggesting that our conclusion is not simply the result of an inability of the fibers to produce higher tensions. Using the protocols of Pate et al. (1994), we find that dissected myofibrilar bundles generate active tensions at 30°C of 0.28 ± 0.02 N/mm^2 (5 observations, average diameter = 22 ± 6 μm), again suggesting that the leveling off of P_o for sufficiently low P_i is not due simply to fiber mechanical instability.

Implications for models of cross-bridge function

With the additional new data that we have obtained at low [P_i], tension now appears to behave as a binding isotherm as a function of the [P_i]. It is important to consider the implications of this behavior in terms of current models of the actomyosin interaction. The free energy of hydrolysis of ATP, ΔG^{ATP}, can be expressed as

$$\Delta G^{ATP} = \Delta G^\circ + kT \ln([ATP]/[ADP][P_i]) \qquad (6)$$

where ΔG° is the standard free energy, k is the Boltzmann constant, and T is absolute temperature. Thus increasing the [P_i] decreases the free energy of hydrolysis of ATP. In terms of the individual states in the actomyosin cycle, this results in those states that precede P_i release, decreasing in free energy relative to those that follow P_i release (Hibberd and Trentham, 1986; Pate and Cooke, 1989a,b). This process is outlined schematically in Fig. 7 *A*, where we assume a single A · M · ADP state. At very low [P_i] the free energy of the A · M · ADP · P_i state lies considerably above that of the A · M · ADP state (as pictured). For sufficiently high [P_i], the free energy of the A · M · ADP · P_i state instead lies below the A · M · ADP state. Letting G_D and G_P be the free energies of the ADP and P_i states, respectively, in units of kT, and letting $\Delta G = G_D - G_P$ be their difference, the fraction, f, of the cross-bridges in the A · M · ADP state as a function of free energy is given by

$$f = \exp(-\Delta G)/[1 + \exp(-\Delta G)] \qquad (7)$$

Assuming for simplicity that the A · M · ADP · P_i state produces no force, with force proportional to the fraction in the A · M · ADP state, the simple force isotherm given by the above ratio of exponential terms is shown as the steepest curve in Fig. 7 *C*. Using Eq. 7, it is straightforward to show that force, as measured by f, decreases from 95% to 5%, for a change in ΔG of 5.9 kT. Then using the relationship between [P_i] and the free energy of hydrolysis of ATP given by Eq. 6, this corresponds to a change of 2.6 units on a log[P_i] scale. In summary, if P_i binds to a single state with a single free energy, the binding isotherm can be titrated by ~2.6 units on a log[P_i] scale.

If the A · M · ADP state(s) occur over a larger range of free energies, then the inhibition of force by P_i would be expected to occur over a larger range of P_i concentrations. Fig. 7 *B* gives a representative case showing four A · M · ADP states, which individually equilibrate with the A · M · ADP · P_i state. This could arise from four distinct isoforms populating the powerstroke, or from four different conformations of a single isoform. We emphasize that we are not postulating the existence of such a powerstroke; rather, we are introducing the idea for explanatory purposes

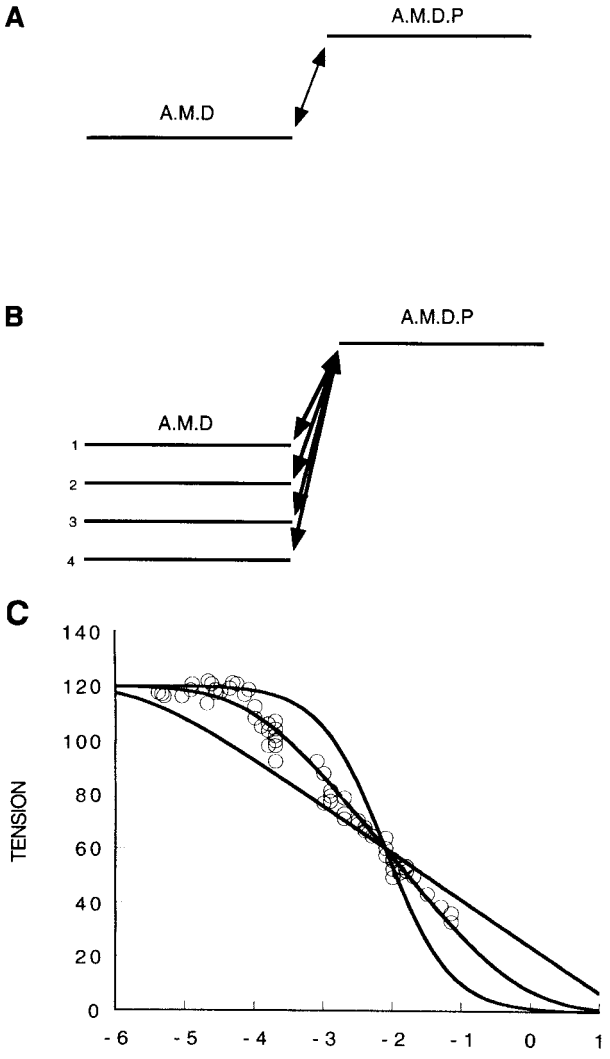

FIGURE 7 Schematic of (*A*) the equilibration between a single A · M · ADP state and an A · M · ADP · P_i state. (*B*) The equilibration between four A · M · ADP states with differing free energies and an A · M · ADP · P_i state. (*C*) Tension was simulated as a function of the $[P_i]$f or a model in which the free energy drop in the powerstroke was varied. The curves are steeper at their midpoints as the free energy in the powerstroke becomes smaller. The curves shown are for free energies of 0 *kT*, 9 *kT*, and 16 *kT*. The data of Fig. 6 are shown and are reasonably fit by a powerstroke with a free energy drop of ~9 *kT*. The curves were simulated using Eqs. 7 and 8.

only. Force will now begin to be inhibited as the energy of the A · M · ADP · P_i state approaches the topmost of the A · M · ADP states; the inhibition will not be complete until the free energy of the A · M · ADP · P_i state decreases to below that of the lowest A · M · ADP state. At the extreme, we may consider the A · M · ADP states to be in a continuous distribution of free energies, as is the case for the linearly elastic cross-bridges of the original, Huxley (1957) cross-bridge model. Following Huxley (1957) and Hill (1974), let $G(x)$ denote this distribution as a function of the spatial distance, x, between cross-bridges and the binding sites, where $x_1 \leq x \leq x_2$. We assume that the A · M · ADP state at the top in the continuum has a free energy of $G(x_2) = G_2$, whereas the A · M · ADP state with minimum free energy occurs at free energy $G(x_1) = G_1$. Thermodynamic consistency requires that the force produced by an attached cross-bridge is dG/dx (Hill, 1974). Then integrating over the fractions attached (Eq. 7), the normalized force, F, produced by a distribution, $p(x)$, of cross-bridges becomes

$$F = \frac{\int_{x_1}^{x_2} \frac{\exp[G_p - G(x)]}{1 + \exp[G_p - G(x)]} p(x)[dG/dx]dx}{\int_{x_1}^{x_2} p(x)[dG/dx]dx}$$

The first integral is the force produced by the fraction in the A · M · ADP state as G_p changes; the second integral is the normalization factor, assuming that all cross-bridges are in the A · M · ADP state. The structure of the integrals allows them to be converted into integrals in G, with the domain of integration becoming $[G_1, G_2]$. Assuming that $p(x)$ is uniform (Huxley, 1957), it cancels out. If the free energy of the A · M · ADP · P_i state is at level G_P, the normalized force, F, can then be evaluated to be

$$F = \frac{\ln[1 + \exp(G_P - G_1)] - \ln[1 + \exp(G_P - G_2)]}{G_2 - G_1} \quad (8)$$

This relationship is also shown in Fig. 7 *C* for the cases where $G_2 - G_1 = 9$ and 16 *kT*, with the larger value for $G_2 - G_1$ resulting in the shallower decrease in tension. As can be seen, the aggregate data of Fig. 6 are well fit by a model in which the free energies of the A · M · ADP states to which P_i binds are spread out over ~9 *kT*.

To facilitate analysis, Eq. 7 was initially discussed in terms of the fraction, f, of cross-bridges in the single A · M · ADP state (Fig. 7 *A*). However, it is straightforward to show that for Eq. 8, the limit of the right-hand side as $G_2 \rightarrow G_1 = G_D$ is identical to the right-hand side of Eq. 7. In other words, Eq. 7 also gives the normalized force, F (the experimental observation of interest), as the single-free-energy A · M · ADP state limit is approached. Subject to integrability constraints, we also note that Eq. 8 is independent of x_1, x_2, and the specific form of $G(x)$ (i.e., the stress-strain relationship for an attached cross-bridge).

We have derived the titration isotherm to be expected for a ligand, P_i, binding to a continuum of states with a continuum of free energies. How do these results relate to current models for the actomyosin interaction and our accumulated data on P_o versus $\log[P_i]$? The A · M · ADP state(s) to which P_i binds are thought to be force-generating states. The magnitude of the $[P_i]$ range necessary to titrate P_o to zero is determined by the requirement that one must titrate the free energy of the pre-powerstroke, A · M · ADP · P_i state(s) down through the powerstroke, A · M · ADP and A · M states, to the end of the powerstroke. This is the free energy minimum of attached, force-producing states. This free energy drop represents the work

that can be done in these states. The analysis of Fig. 7 indicates that this free energy drop is ~9*kT*. The question becomes whether 9*kT* is sufficient free energy to drive the powerstroke.

The mechanical energy that is produced in the powerstroke can be estimated from measurements of the efficiency (the ratio of mechanical work produced divided by the free energy consumed by the actomyosin interaction) of active muscles. Experimentally, the chemomechanical efficiency of contracting muscle is been observed to be ~60% (Woledge et al., 1985). For the ligand concentrations found interior to muscle cells, the free energy of ATP hydrolysis is 23*kT*. This implies that ~14*kT* of the free energy of hydrolysis of ATP (0.6 × 23) can be converted into work. More complex, multistate, chemomechanical models that also include the resistive drag forces from negatively strained cross-bridges in intermediate states in the contractile cycle have suggest that reasonable efficiency requires an upward adjustment of the 14*kT* value to ~18*kT* (Eisenberg et al., 1980; Pate and Cooke, 1989b).

The drop of 14–18*kT* in free energy occurring in the powerstroke was somewhat larger than the 9*kT* suggested by our data. However, our experiments were done at 10°C, well below the 39°C internal, physiological temperature of a rabbit. The efficiency of rabbit psoas muscle at 10°C is not known. Isometric tension increases as temperature increases above 10°C, with a Q_{10} of 1.4 previously determined over the range 10°C to 30°C (Pate et al., 1994). How will the data of Fig. 6 change if taken at physiological temperatures? Dantzig et al. (1992) have investigated the temperature dependence of the decrease in P_o with [P_i] at 10°C and 20°C. Plotting P_o versus log[P_i] (their Fig. 1), they observed roughly the same slope for the decrease in P_o at the two temperatures. If the slope of the P_o versus log[P_i] plot remains unchanged as temperature increases, extrapolation of the data of Fig. 6 (assuming a breakpoint at 100 μM [P_i]) to 39°C corresponds to a free energy change of 18*kT*. This value is comparable to that suggested by efficiency considerations. This analysis obviously has its limitations, but is clearly consistent with the idea that the smaller free energy drop in the powerstroke that we observe is a result of the experimental temperature employed.

We conclude that the titration of force with P_i shows that there is a large free energy drop in the A · M · ADP state(s) to which P_i binds. This free energy drop is of the right magnitude to explain the observed mechanics and energetics of fiber contraction. It is possible that force is also produced in other states, e.g., before P_i release, but titration of force to less than ~30% of maximum shows that 70% or more of the force is generated in the A · M · ADP states to which P_i binds.

This work was supported by U.S. Public Health Service grants HL 32145 (RC) and AR39643 (EP), and a grant from the Muscular Dystrophy Association (RC).

REFERENCES

Altringham, J., and I. A. Johnston. 1985. Effects of phosphate on the contractile properties of fast and slow muscle fibres from an Antarctic fish. *J. Physiol. (Lond.).* 368:491–500.

Brune, M., J. L. Hunter, J. E. T. Corrie, and M. R. Webb. 1994. Direct, real-time measurement of rapid inorganic phosphate release using a novel fluorescent probe and its application to actomyosin subfragment1 ATPase. *Biochemistry.* 33:8262–8271.

Chase, P. B., and M. J. Kushmerick. 1988. Effects of pH on contraction of rabbit fast and slow skeletal muscle fibers. *Biophys. J.* 53:935–946.

Cooke, R. 1986. The mechanism of muscle contraction. *CRC Crit. Rev. Biochem.* 21:53–118.

Cooke, R., and W. Bialek. 1979. Contraction of glycerinated muscle fibers as a function of the ATP concentration. *Biophys. J.* 28:241–258.

Cooke, R., K. Franks, G. Luciani, and E. Pate. 1988. The inhibition of rabbit skeletal muscle contraction by hydrogen ions and phosphate. *J. Physiol. (Lond.).* 395:77–97.

Cooke, R., and I. D. Kunz. 1974. The properties of water in biological systems. *Annu. Rev. Biophys. Bioeng.* 3:95–126.

Cooke, R., and E. Pate. 1985. The effects of ADP and phosphate on the contraction of muscle fibers. *Biophys. J.* 48:789–798.

Dantzig, J. A., Y. E. Goldman, J. Lacktis, N. C. Millar, and E. Homsher. 1992. Reversal of the cross-bridge force generating transition by photogeneration of phosphate in rabbit psoas muscle fibres. *J. Physiol. (Lond.).* 451:247–278.

Eisenberg, E., T. L. Hill, and Y. Chen. 1980. Cross-bridge model of muscle contraction. *Biophys. J.* 29:195–227.

Franks, K., and R. Cooke. 1980. All myosin heads form bonds with actin in rigor rabbit skeletal muscle. *Biochemistry.* 19:2265–2269.

Franks-Skiba, K., T. Hwang, and R. Cooke. 1994. Quenching of fluorescent nucleotides bound to myosin: a probe of the active-site conformation. *Biochemistry.* 33:12720–12728.

Hibberd, M. G., J. A. Dantzig, D. R. Trentham, and Y. E. Goldman. 1985. Phosphate release and force generation in skeletal muscle fibers. *Science.* 228:1317–1319.

Hibberd, M. G., and D. R. Trentham. 1986. Relationships between chemical and biochemical events during muscular contraction. *Annu. Rev. Biophys. Biophys. Chem.* 15:119–161.

Hill, T. L. 1974. Theoretical formalism for the sliding filament model of contraction of striated muscle, Part I. *Prog. Biophys. Mol. Biol.* 28: 267–340.

Huxley, A. F. 1957. Muscle structure and theories of contraction. *Prog. Biophys.* 7:255–318.

Kawai, M. 1986. The role of orthophosphate in crossbridge kinetics in chemically skinned rabbit psoas fibres as detected with sinusoidal and step length alterations. *J. Muscle Res. Cell Motil.* 7:421–434.

Kawai, M., K. Guth, K. Winnikes, C. Haist, and J. C. Ruegg. 1987. The effect of inorganic phosphate on the ATP hydrolysis rate and the tension transients in chemically skinned rabbit psoas fibers. *Pflügers Arch.* 408:1–9.

Kawai, M., and H. R. Halvorson. 1989. Role of MgATP and MgADP in the cross-bridge kinetics in chemically skinned rabbit psoas fibers. Study of a fast exponential process (C). *Biophys. J.* 55:595–603.

Kawai, M., and H. R. Halvorson. 1991. Two step mechanism of phosphate release and the mechanism of force generation in chemically skinned fibers of rabbit psoas muscle. *Biophys. J.* 59:329.

Krenitsky, T. A., G. B. Elion, A. M. Henderson, and G. H. Hitchings. 1968. Inhibition of human purine nucleoside phosphorylase. Studies with intact erythrocytes and the purified enzyme. *J. Biol. Chem.* 243: 2876–2881.

Kulikowska, E., A. Bzowska, J. Wierzchowski, and D. Shugar. 1986. Properties of two unusual, and fluorescent, substrates of purine-nucleoside phosphorylase: 7-methylguanosine and 7-methylinosine. *Biochim. Biophys. Acta.* 874:355–363.

Mannherz, H. G. 1968. ATP-spalting and ATP-diffusion in oscillierenden extra hierten muskolfasern. *Pflügers Arch.* 303:230–248.

Marston, S. B. 1973. The nucleotide complexes of myosin in glycerol-extracted muscle fibers. *Biochim. Biophys. Acta.* 305:397–412.

Martyn, D. A., and A. M. Gordon. 1992. Force and stiffness in glycerinated rabbit psoas fibers: effects of calcium and elevated phosphate. *J. Gen. Physiol.* 99:795.

Mieyal, J. J., and R. H. Abeles. 1972. Disaccharide phosphorylases. *In* The Enzymes, Vol. 7. P. D. Boyer, editor. Academic Press, New York. 515–532.

Millar, N. C., and E. Homsher. 1990. The effect of phosphate and calcium on force generation in glycerinated rabbit skeletal muscle fibers. A steady state and transient kinetic study. *J. Biol. Chem.* 265: 20234–20240.

Murakami, K., A. Mitsui, and K. Tsushima. 1971. Purine nucleoside phosphorylase of chicken liver. *Biochim. Biophys. Acta.* 235:99–105.

Naylor, G. R. S., E. M. Bartels, T. D. Bridgman, and G. F. Elliot. 1985. Donnan potentials in rabbit psoas muscle in rigor. *Biophys. J.* 48:47–59.

Parks, R. E., and R. P. Agarwal. 1972. Purine nucleoside phosphorylase. *In* The Enzymes, Vol. 7. P. D. Boyer, editor. Academic Press, New York. 483–514.

Pate, E., and R. Cooke. 1988. Energetics of the actomyosin bond in the filament array of muscle fibers. *Biophys. J.* 53:561–573.

Pate, E., and R. Cooke. 1989a. Addition of phosphate to active muscle fibers probes actomyosin states within the powerstroke. *Pflügers Arch.* 414:73–81.

Pate, E., and R. Cooke. 1989b. A model of crossbridge action: the effects of ATP, ADP, and P_i. *J. Muscle Res. Cell Motil.* 10:181–196.

Pate, E., K. L. Nakamaye, K. Franks-Skiba, and R. Cooke. 1991. Mechanics of glycerinated muscle fibers using nonnucleoside triphosphate substrates. *Biophys. J.* 59:598–605.

Pate, E., G. Wilson, M. Bhimani, and R. Cooke. 1994. Temperature dependence of the inhibitory effects of orthovanadate on shortening velocity in fast skeletal muscle. *Biophys. J.* 66:1554–1562.

Porter, D. J. T. 1992. Purine nucleoside phosphorylase. Kinetic mechanism of the enzyme from calf spleen. *J. Biol. Chem.* 267:7342–7351.

Rayment, I., H. M. Holden, M. Whittaker, C. B. Yohn, M. Lorenz, K. C. Holmes, and R. A. Milligan. 1993a. Structure of the actin-myosin complex and its implications for muscle contraction. *Science.* 261: 58–65.

Rayment, I., W. R. Rypniewski, K. Schmidt-Base, R. Smith, D. R. Tomchick, M. M. Benning, D. A. Winkelmann, G. Wesenberg, and H. M. Holden. 1993b. Three-dimensional structure of myosin subfragment-1: a molecular motor. *Science.* 261:50–57.

Ropp, P. A., and T. W. Traut. 1991. Allosteric regulation of purine nucleoside phosphorylase. *Arch. Biochem. Biophys.* 288:614–620.

Seow, C. Y., and L. E. Ford. 1997. Exchange of ATP for ADP on high force cross-bridges of skinned rabbit muscle fibers. *Biophys. J.* 72: 2719–2735.

Sleep, J., and H. Glyn. 1986. Inhibition of myofibrillar and actomyosin subfragment 1 adenosinetriphosphatase activity by adenosine 5′-diphosphate and adenyl 5′-yl imidodiphosphate. *Biochemistry.* 25: 1149–1154.

Taylor, E. W. 1979. Mechanism of actomyosin ATPase and the problem of muscle contraction. *CRC Crit. Rev. Biochem.* 6:103–164.

Walker, J. W., and R. L. Moss. 1992. Effects of Ca^{2+} on the kinetics of phosphate release in skeletal muscle. *J. Biol. Chem.* 267:2459–2466.

Webb, M. R. 1992. A continuous spectrophotometric assay for inorganic phosphate and for measuring phosphate release kinetics in biological systems. *Proc. Natl. Acad. Sci. USA.* 89:4884–4887.

Woledge, R. C., N. A. Curtin, and E. Homsher. 1985. Energetic Aspects of Muscle Contraction. Academic Press, London.

Yoshizaki, K., Y. Seo, H. Nishikawa, and T. Morimoto. 1982. Application of pulsed-gradient ^{31}P NMR on frog muscle to measure the diffusion rates of phosphorous compounds in cells. *Biophys. J.* 38:209–211.

Yount, R. G., D. Lawson, and I. Rayment. 1995. Is myosin a "back door" enzyme? *Biophys. J.* 68:44s.

Zimmerman, T. P., N. Gerstein, A. F. Ross, and R. P. Miech. 1971. Adenine as a substrate for purine nucleoside phosphorylase. *Can. J. Biochem.* 49:1050–1054.